NREL
NATIONAL RENEWABLE ENERGY LABORATORY

A Detailed Physical Trough Model for NREL's Solar Advisor Model

Preprint

Michael J. Wagner, Nate Blair, and Aron Dobos
National Renewable Energy Laboratory

To be presented at SolarPACES 2010
Perpignan, France
September 21-24, 2010

Conference Paper
NREL/CP-5500-49368
October 2010

Contract No. DE-AC36-08GO28308

Available electronically at http://www.osti.gov/bridge

Available for a processing fee to U.S. Department of Energy
and its contractors, in paper, from:

U.S. Department of Energy
Office of Scientific and Technical Information

P.O. Box 62
Oak Ridge, TN 37831-0062
phone: 865.576.8401
fax: 865.576.5728
email: mailto:reports@adonis.osti.gov

Available for sale to the public, in paper, from:

U.S. Department of Commerce
National Technical Information Service
5285 Port Royal Road
Springfield, VA 22161
phone: 800.553.6847
fax: 703.605.6900
email: orders@ntis.fedworld.gov
online ordering: http://www.ntis.gov/help/ordermethods.aspx

Cover Photos: (left to right) PIX 16416, PIX 17423, PIX 16560, PIX 17613, PIX 17436, PIX 17721

Printed on paper containing at least 50% wastepaper, including 10% post consumer waste.

SolarPACES 2010

A DETAILED PHYSICAL TROUGH MODEL FOR NREL'S SOLAR ADVISOR MODEL

Michael J. Wagner[1], Nate Blair[2], Aron Dobos[3]

[1]Mechanical Engineer, National Renewable Energy Laboratory, Golden, Colorado (USA)
Email: michael.wagner@nrel.gov, Phone: +1.303.384.7430

[2]Senior Energy Analyst, Group Manager, National Renewable Energy Laboratory

[3]Programming Engineer, National Renewable Energy Laboratory

1 Introduction

Solar Advisor Model (SAM) [1] is a free software package made available[1] by the National Renewable Energy Laboratory (NREL)[2], Sandia National Laboratory, and the US Department of Energy. SAM contains hourly system performance and economic models for concentrating solar power (CSP) systems, photovoltaic, solar hot-water, and generic fuel-use technologies. Versions of SAM prior to 2010 included only the parabolic trough model based on Excelergy [2]. This model uses top-level empirical performance curves to characterize plant behavior, and thus is limited in predictive capability for new technologies or component configurations. To address this and other functionality challenges, a new trough model derived from physical first principles was commissioned to supplement the Excelergy-based empirical model. This new "physical model" approaches the task of characterizing the performance of the whole parabolic trough plant by replacing empirical curve-fit relationships with more detailed calculations where practical. The resulting model matches the annual performance of the SAM empirical model (which has been previously verified with plant data) while maintaining run-times compatible with parametric analysis, adding additional flexibility in modeled system configurations, and providing more detailed performance calculations in the solar field, power block, piping, and storage subsystems.

2 Model formulation

This work introduces several new parabolic trough modeling capabilities into SAM. These include (1) a power block model that is responsive to variations in ambient temperature, inlet HTF mass flow rate and temperature, boiler pressure, and cooling technology, (2) a solar field model that allows variation in receiver geometry, absorber surface properties, and loop configuration, (3) a water-use model that accounts for steam cycle blow-down, mirror washing, and evaporative cooling loss, and (4) a two-tank storage model that tracks volume and temperature, adjusts for thermal losses, and accounts for heat exchanger temperature degradation. The discussion in this paper considers model capabilities and formulations in greater detail.

2.1 Solar Field

The solar field is the heat-collecting portion of the plant. It consists of one or more loops of solar collector assemblies (SCA's), with each loop laid out in parallel. A common header pipe provides each loop with an equal flow rate of heat transfer fluid (HTF), and a second header collects the hot HTF to return it to the power block directly for power generation or to thermal storage for use at a later time. The model's configuration allows the user to provide unique collector and receiver properties for each SCA in the loop. The solar field model is conceptually segregated into a top-level energy formulation and lower-level

[1]Available via download at `www.nrel.gov/analysis/sam`

[2]The Alliance for Sustainable Energy, LLC (Alliance), is the manager and operator of the National Renewable Energy Laboratory (NREL). Employees of the Alliance, under Contract No. DE-AC36-08GO28308 with the U.S. Dept. of Energy, have authored this work.

subsystem models for the collector, receiver, and non-absorbing piping.

2.1.1 Energy equations

Each SCA is composed of a number of parabolic collectors and associated receivers in series that share a single common tracking drive. The SCA is treated as an independent calculation node within the loop, so the absorbed energy, losses, temperature, pressure drop, and other performance values are calculated independently for each SCA. This allows each SCA to contain different receiver and/or collector attributes and have a user-assigned defocusing order. The nodal approach is illustrated in Figure 1.

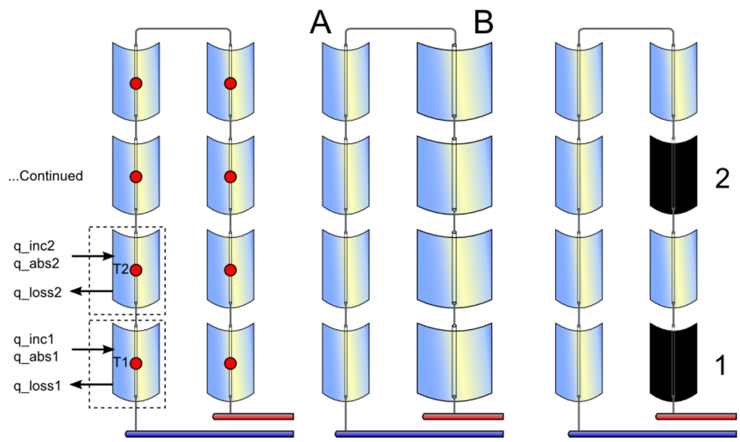

Figure 1: The nodal structure of the loop is shown (left) where each SCA in the loop is an autonomous node. This framework allows multiple receiver/collector types - shown as A and B (center) - and user-specified defocusing schemes (right).

A steady-state trough receiver model determines the temperature rise across the node with an energy balance between the absorbed energy, the mass flow rate of HTF through the receiver, and the specific heat of the HTF. However, a steady-state model is insufficient once the thermal inertia associated with the energy state becomes significant. This is the case for parabolic troughs so transient terms must be included. The most significant transient effect in the solar field is the thermal mass of the HTF in the headers and in the receiver piping, so the analytical formulation must account for the change in energy of the HTF. The general solution to the energy balance equation for a single node is shown in Eq.[1], where $\dot{m}_{htf}$ is the HTF mass flow rate, $\dot{q}_{abs}$ is the absorbed thermal energy, c_{htf} is the HTF specific heat, m is the HTF mass in the node, T_{in} is the incoming HTF temperature, T is the temperature of the node at time t, and Δt is the timestep duration.

$$T = \frac{\dot{q}_{abs}}{\dot{m}_{htf} \cdot c_{htf}} + C_1 e^{-\frac{\dot{m}_{htf}}{m}\Delta t} + T_{in} \tag{1}$$

This equation has an unknown constant C_1 that can be determined by enforcing a boundary condition. In this situation, we know that the temperature $T = T_0$ at the beginning of the timestep when $t = 0$, and we define T_0 to be the temperature at the end of the previous timestep. Solving for the unknown constant C_1 and substituting back into the general solution:

$$T_i = \frac{\dot{q}_{abs,i}}{\dot{m}_{htf}\; c_{htf,i}} + \left(T_{0,i} - \frac{\dot{q}_{abs,i}}{\dot{m}_{htf}\; c_{htf,i}} - T_{i-1}\right) e^{\frac{\dot{m}_{htf}}{m_i}\Delta t} + T_{i-1} \tag{2}$$

This equation is applied to each node i in the loop, where $T_{in,i}$ is equal to the outlet temperature of the previous node in the loop, T_{i-1}. Since the calculated temperature for each node depends on both the inlet temperature of the previous node and the node temperature from the previous timestep, these values must be established as boundary conditions. The temperature of the node at the previous timestep is simply tracked and stored from timestep to timestep to satisfy this requirement, and the inlet temperature can be set equal to the outlet temperature of the previous node for each but the first node in the loop.

The inlet and outlet field temperatures incorporate the thermal inertia of the header HTF in calculating the respective temperatures. Under steady-state conditions, the loop inlet HTF temperature equals either the power block outlet temperature, the storage loop outlet temperature, or the solar field outlet temperature, depending on the control situation. However, using any of these outlet temperatures as the loop inlet value is inaccurate because it fails to account for the thermal inertia of the header. Including thermal inertia as a transient effect, the derived equation for loop inlet temperature (denoted $T_{sys,c}$) is shown in Eq.[3].

$$T_{sys,c} = (T_{sys,c,0} - T_{in})\, e^{-\frac{\dot{m}_{htf}}{\overline{V}_c \cdot \rho_c} \Delta t} + T_{in} \tag{3}$$

$$T_{sys,h} = (T_{sys,h,0} - T_{out})\, e^{-\frac{\dot{m}_{htf}}{\overline{V}_h \cdot \rho_h + \frac{mc_{bal}}{c_h}} \Delta t} + T_{out} \tag{4}$$

Here, the cold header temperature from the last timestep is $T_{sys,c,0}$, the volume in the cold header and the runner pipe is given by $\overline{V}_c$, and cold fluid density is ρ_c. Analogously, the hot system outlet temperature combines loop outlet flow, the header and runner pipe volumes, and the state of the system at the last timestep, but one additional parameter is included: mc_{bal}. This term adds flexibility for the user to account for non-HTF thermal inertia in the specification of the system. This term may include pipe walls, insulation, the expansion vessel, heat exchanger mass, and other sources of thermal inertia.

2.1.2 Collectors and field optics

The collector model and optical calculations used in the physical trough model are largely borrowed from the SAM empirical collector model. The collector is the portion of the solar field that reflects incoming irradiation onto the receiver. This equipment is distinct from the receiver component that consists of an evacuated glass envelope and tube receiver. The optical calculations for the collector model extend to the point of determining the magnitude of solar flux that is incident on the receiver.

Both fixed derate-type losses and variable losses that change with solar position are considered to determine the flux incident on the receiver. When the solar irradiation is not normal to the plane of the collector aperture, losses are incurred that scale with the severity of incidence angle. The incidence angle θ is equal to the angular difference between the normal to the aperture plane and the incoming solar irradiation. SAM calculates this value based on the collector tracking angle (ω_{col}) at a given solar azimuth (γ_s) and elevation angle (θ_e), where the collector orientation with an azimuth angle (γ_{col}) and a tilt angle (θ_{col}) that is positive when the portion of the field closet to the equator is tilted up [3]. The incidence angle θ is determined using the tracking angle and orientation information.

$$\theta = \cos^{-1} \sqrt{1 - [\cos(\theta_e - \theta_{col}) - \cos(\theta_{col})\ \cos(\theta_e)\ (1 - \cos(\gamma_s - \gamma_{col}))]^2} \tag{5}$$

The solar position-dependent optical losses accounted for in this model are the cosine loss in Eq.[6], end spillage in Eq.[7], stow and deploy angle limitations, incidence angle modifier in Eq.[8], and row-to-row shadowing in Eq.[9]. These equations make use of the average focal length ($L_{f,ave}$), the number of solar collector assemblies per loop (N_{sca}), the axis-to-axis distance between collector rows ($L_{spacing}$), aperture width (w), and the collector length (L_{col}).

$$\eta_{cos} = \cos(\theta) \tag{6}$$

$$\eta_{endLoss} = 1 - L_{f,ave}\ \tan(\theta) - \left(\frac{N_{sca}}{2} - 1\right) \frac{2 \cdot (L_{f,ave}\ \tan(\theta) - L_{spacing})}{N_{sca} \cdot L_{col}} \tag{7}$$

$$\eta_{IAM} = a_0 + a_1 \frac{\theta}{\cos\theta} + a_2 \frac{\theta^2}{\cos\theta} \quad \rightarrow (\theta \; in \; radians) \tag{8}$$

$$\eta_{shadow} = |\sin(90^\circ - \omega_{col})| \, \frac{L_{spacing}}{w} \tag{9}$$

The trough collector model captures optical efficiency with losses that are a function of solar position and with fixed losses that are applied as constant multipliers. Fixed losses include tracking error, geometry defects, mirror reflectance, mirror soiling, and general error not captured by the other items. Total optical efficiency is thus equal to the product of all efficiency terms as shown in Eq.[10], and the total radiative energy incident on the solar field is calculated in Eq.[11] by multiplying the efficiency by the beam normal irradiation (I_{bn}) and the total solar field aperture area ($A_{ap,tot}$).

$$\eta_{opt}(\theta, \omega_{col}) = \eta_{endLoss}(\theta) \; \eta_{shadow}(\omega_{col}) \; \eta_{IAM}(\theta) \; \eta_{track} \; \eta_{geo} \; \rho_m \; \eta_{soil} \; \eta_{gen} \tag{10}$$

$$\dot{q}_{inc,sf} = I_{bn} \; A_{ap,tot} \; \eta_{opt}(\theta, \omega_{col}) \tag{11}$$

2.1.3 Receivers

The receiver model in the physical trough uses a 1-dimensional heat transfer model presented by Forristall in detail in [4]. Receiver heat loss is highly dependent on surface temperature, while the surface temperature is influenced by the absorbed thermal energy and the subsequent heat loss. The receiver model contains numerous implicit relationships between temperature, heat loss, and substance properties. SAM solves these implicit equations iteratively using successive substitution until the surface temperatures converge.

The receiver is modeled as a 1-dimensional energy flow where only the temperature gradient in the radial direction is assumed to be significant - axial and circumferential temperature gradients are neglected. Figure 2 presents a diagram of one quarter of the receiver in cross-section. Each temperature T_{1-5} is calculated by the model using an energy balance and temperature-dependent loss coefficients. The receiver geometry is specified by the user with radii R_{1-4}.

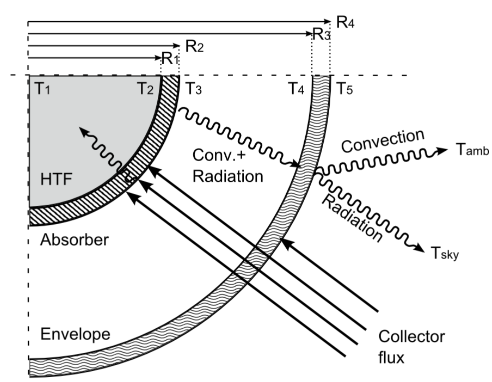

Figure 2: A heat balance for the modeled receiver. Heat transfer in the radial direction (left to right) is considered, while circumferential and axial transfer is not.

Concentrated irradiative flux from the collector passes through the transparent glass envelope (R_{3-4}) where a small fraction is absorbed. This absorption fraction is specified by the user as *envelope absorptance* (α_{env}) on the Receivers page, and influences the calculated temperature of the glass. The unabsorbed irradiation strikes the absorber tube at R_2. Note that the fraction of energy passing through the glass envelope is specified by the *envelope transmittance* value on the Receivers page, and need not equal the complement of the absorptance value.

During operation, the heated surface at R_2 drives thermal energy through the absorber wall (R_{1-2}) and into the HTF. Thermal losses from the absorber surface occur via convection and radiation exchange with the glass envelope, and the glass envelope is in turn exposed to ambient air. Figure 3 shows the heat transfer network, conceptualized as a set of thermal resistances in series and parallel. This is analogous to an electrical resistance network where thermal energy represents current, thermal resistance represents electrical resistance, and temperature drop is equivalent to voltage drop. Incidentally, the same resistance formulae apply to thermal and electrical networks.

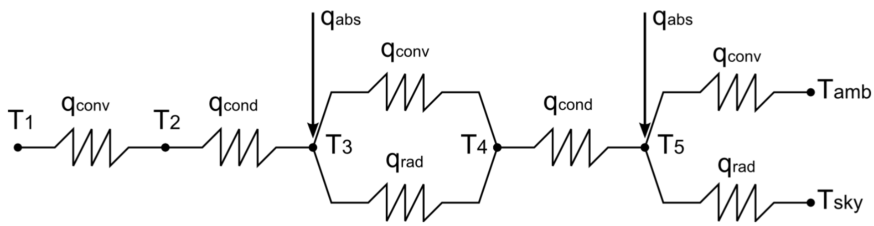

Figure 3: The thermal resistance network for the receiver model shown in 2. Energy is absorbed at T_3 and T_{4-5}.

The total heat loss from the tube is expressed in terms of thermal resistances by applying resistance network rules to the section of Figure 3 between T_3 and the ambient temperatures. Each $\hat{R}$ value physically represents thermal resistance to heat transfer via conduction, convection, or radiation, and has units of $^{W}/_{K}$.

$$
\begin{aligned}
\dot{q}_{hl} &= \frac{(T_3 - T_{amb})\,\hat{R}_{57,rad} + (T_3 - T_{sky})\,\hat{R}_{56,conv} - \dot{q}_{abs,env}\,\Omega_{\hat{R}}}{\hat{R}_{34,tot}\,\hat{R}_{57,rad} + \hat{R}_{34,tot}\,\hat{R}_{56,conv} + \Omega_{\hat{R}}} \qquad (12)\\
where:&\\
\Omega_{\hat{R}} &= \hat{R}_{56,conv}\,\hat{R}_{57,rad} + \hat{R}_{45,cond}\,\hat{R}_{57,rad} + \hat{R}_{45,cond}\,\hat{R}_{56,conv}
\end{aligned}
$$

This equation is somewhat simplified as the envelope resistances drop out in the case that the receiver glass is removed/broken and the absorber surface is in direct thermal communication with the ambient.

$$\dot{q}_{hl} = (T_3 - T_6)\,\hat{R}_{34,conv} + (T_3 - T_7)\,\hat{R}_{34,rad} \qquad (13)$$

2.1.4 Piping model

The largest parasitic loss for a trough plant is the electricity consumed by the solar field HTF pumps. Since pumping power scales proportionally with the HTF pressure drop across the solar field and with the HTF mass flow rate, accurately capturing both of these values is important in characterizing the total plant performance. The piping performance model in SAM is derived directly from work presented in [5]. Diameter selection for runner and header piping applies an HTF velocity limitation for the design-point HTF mass flow rate to ensure that the selected pipe diameter falls within a user-supplied maximum and minimum velocity.

The piping model in SAM accounts for the pressure drop associated with a variety of field components, including “runner” piping to and from the solar field headers, hot and cold headers, receiver tube piping, pipe expansions and contractions, elbows (long, medium, standard), valves (gate, globe, check, and control), and ball joint assemblies. The piping model keeps track of the total fluid volume and surface area of the piping, excepting the surface area of the receiver absorber tubing. The model does not account for varying insulation thickness, but instead applies an area/temperature-specific heat loss coefficient to determine the total thermal energy loss from piping.

2.2 Power block

The ultimate goal of the power block model is to accurately characterize off-design performance while providing enough flexibility to handle typical steam Rankine cycle designs. Detailed process modeling software packages often provide this capability but often require extensive setup and long run-times, presenting practical challenges for implementation in the TRNSYS framework. Instead of incorporating a detailed model directly into TRNSYS, process-simulation software is used to construct a representative detailed cycle, and the output from part-load parametric simulations is converted into an off-design performance response surface. SAM uses an adaptation of the well-known "design of experiments" statistical approach [6] to characterize variable dependencies and generate the response surfaces. This specific approach is originally described in [7] and expanded in [8]. The procedure used for developing a regression model from more detailed performance calculations is summarized as follows:

- Practical limits on the range of the three independent variables are identified. The variables are (A) HTF inlet temperature, (B) Condenser pressure, and (C) HTF mass flow rate
- Parametric runs evaluate the gross power output ($\dot{W}$) and power block heat input ($\dot{Q}$) over the full range of inputs.
- The information generated by parametric runs in detailed modeling software is non-dimensionalized.
- Non-dimensional information is analyzed to determine the main effects and effect interactions.
- These effects are consolidated and applied in the code.

2.2.1 *Heat rejection*

The two cooling technologies available to nearly all CSP plants are wet cooling and dry cooling. These technologies lie on opposite ends of the spectrum in terms of both performance and water use [9], and these are the technologies that SAM models[3].

Both wet and dry cooling use ambient air as the ultimate cold thermal reservoir, but differ in the mechanism of heat transfer between the cycle and air. Wet cooling systems use a deluge of water to remove heat through evaporation; thus the temperature of the cold reservoir is driven by the wet-bulb temperature. Dry cooling systems transfer heat directly from the steam working fluid to air using a sensible-heat process. This technique is limited by the dry-bulb temperature of air, which can be significantly higher than the wet bulb temperature, especially in arid regions where CSP is most desirable. The heat rejection models in SAM account for the performance impact of variation in ambient temperature, parasitic consumption of associated fans and pumps, and water use in the case of the wet cooling system.

2.3 Thermal storage

CSP is unique among renewable technologies in it's ability to divert and cost-effectively store energy for later use in a thermal energy storage (TES) system. Storage allows for uninterrupted power production during temporary weather transients, shifting the operating hours to match peak demand, generally increasing the capacity factor of the plant, or supplying low-level heat to plant processes that require it (like maintaining the power block in a standby mode). Solar Advisor models thermal storage for a two-tank system; that is, two tanks each are capable of holding the entire HTF volume for thermal storage. Both the hot and cold tanks use the same tank model to simulate their behavior, though the inputs and outputs for each are managed separately. The tank model is based on a methodology similar to what is used for the variable-volume tank (Type 39) in the standard TRNSYS library [10]. SAM also models a solar-field-to-storage heat exchanger for indirect systems using an effectiveness-NTU approach [11].

[3] A parallel wet/dry hybrid cooling model is forthcoming in SAM in the Fall of 2010.

2.4 Auxiliary heater

A fossil-fired auxiliary heater is included in some systems to supply thermal energy during times of no solar resource or when storage cannot fully meet the required load. SAM models a simple fossil-fuel burning auxiliary heater that generates heat for use in power production. It is automatically limited to a maximum heating rate equal to the power block design thermal input. SAM uses the lower heating value (LHV) efficiency to estimate fuel energy content and fuel usage.

2.5 Plant control

The plant controller links the user's input with the requirements of the power block and the resource production available from the solar field, thermal storage, and auxiliary heater. The controller also impacts how and when the solar field is used. SAM uses four main operating modes including (1) total available solar field energy output is less than the usable minimum, (2) total energy is between the minimum and the design-point power block load, (3) more energy is produced than can be used in the power block or storage (if the system has storage), and (4) more energy is available than the power block needs, but all of the remainder can be diverted to storage.

The controller calculates the solar field inlet temperature based on the performance of the various plant subsystems, including the solar field using an iterative process. The field inlet temperature is determined by a weighted average of the power block mass flow and the TES charge mass flow.

$$T_{sf,in} = \frac{\dot{m}_{pb}\, T_{pb,out} + \dot{m}_{chg}\, T_{tes,cold}}{\dot{m}_{pb} + \dot{m}_{chg}} \tag{14}$$

For cases where the power block is not in operation and thermal storage is not being charged (i.e. $\dot{m}_{pb} + \dot{m}_{chg} = 0$), the solar field inlet temperature is equal to the solar field outlet temperature. Convergence is achieved when either the convergence error doesn't change from iteration to iteration, or when the convergence error itself falls below the specified tolerance.

2.6 Parasitics

Solar Advisor uses several different approaches to model parasitic losses. These include the detailed approach for the piping model and the power block parasitics as well as more general coefficient-based methods. Table 1 lists the parasitic loss items accounted for, their corresponding subsystem, and the modeling approach.

	Loss	**Subsystem**	**Modeling Approach**
1.	SCA drives & electronics	Solar field	Coefficient-based calculation
2.	Solar field HTF pumps	Solar field	Detailed performance model
3.	Piping freeze protection	Solar field	Detailed performance model
4.	Power block HTF pump	Controller	Coefficient-based calculation
5.	Storage HTF pump	Controller	Coefficient-based calculation
6.	Fixed parasitic losses	Controller	Constant fractional loss
7.	Balance of plant parasitics	Controller	Polynomial curve with coefficients
8.	Auxiliary heater operation	Controller	Polynomial curve with coefficients
9.	Heat rejection equipment	Power block	Detailed performance model
10.	Storage heat trace heater	Thermal storage	Detailed performance model

Table 1: A summary of the parasitic losses accounted for by SAM

3 Model verification

Performance of this model has been compared to the SAM empirical trough for several system configurations. In general, the models compare very well, with differences in annual output for analogous systems of less than 1.5%. Table 2 shows the annual output metrics for a wet-cooled 100MW-net trough system with 6 hours of thermal storage as modeled with the two SAM trough models.

Metric	Units	Phys. Model	Emp. Model	Difference
Total incident solar radiation	GW-hr	2,384.1	2,384.1	0%
Thermal energy from solar field	GW-hr	1,164.6	1,220.8	-4.6%
Thermal energy to power block	GW-hr	1,134.3	1,145.8	-1.0%
Power cycle gross output	GW-hr	419.0	429.9	-2.5%
Net electric output	GW-hr	379.3	384.3	-1.1%

Table 2: Results of a comparison between this model and the empirical trough model in SAM

4 Summary

The SAM physical parabolic trough plant model fulfills several goals besides deriving system performance from first principles. Namely, the model includes transient effects related to the thermal capacity of the HTF in the field piping, headers, and the balance of the plant, it allows for more flexible receiver and collector specification, it maintains a reasonably short run-time (10-20 seconds/annum) conducive to parametric and statistical analysis, and it makes use of previously existing subcomponent models where possible. The models that are adapted and incorporated into the physical model include the receiver heat loss model by [4], the empirical collector model, a field piping pressure drop model by [5], and the power block performance model developed by [7] for the power tower system model in SAM. As demonstrated in Table 2, the system model performance agrees well with the validated empirical model.

References

[1] P. Gilman. Solar Advisor Model User Manual. Technical report, National Renewable Energy Laboratory, Golden, Colorado (USA), April 2010.

[2] N. Blair, M. Mehos, and C. Christensen. Sensitivity of concentrating solar power trough performance, cost, and financing with the Solar Advisor Model. Las Vegas, Nevada, USA, March 2008. Proceedings of the SolarPACES International Symposium.

[3] W. Stine and M. Geyer. *Power from the Sun.* Published online at www.powerfromthesun.net, 2001.

[4] R. Forristall. Heat transfer analysis and modeling of a parabolic trough solar receiver implemented in engineering equation solver. Technical Report NREL/TP-550-34169, National Renewable Energy Laboratory, Golden, Colorado, USA, 2003.

[5] B. Kelly and D. Kearney. Parabolic trough solar system piping model: Final report. Technical Report NREL/SR-550-40165, National Renewable Energy Laboratory, Golden, Colorado, USA, 2006.

[6] C.F.J. Wu and M. Hamada. *Experiments: Planning, Analysis, and Parameter Design Optimization.* Wiley, 2000.

[7] M. Wagner. Simulation and predictive performance modeling of utility-scale central receiver system power plants. Master's thesis, University of Wisconsin, Madison, Wisconsin, USA, 2008.

[8] M. Wagner. Methodology for constructing reduced-order powerblock performance models for csp applications. Perpignon, France, 2010. Proceedings of the SolarPACES International Symposium, SolarPACES. Publication pending.

[9] M. Wagner and C. Kutscher. The impact of hybrid wet/dry cooling on concentrating solar power plant performance. Phoenix, Arizona, USA, 2010. Proceedings of the 4th International Conference on Energy Sustainability, ASME.

[10] Solar Energy Lab, University of Wisconsin - Madison. *TRNSYS 16: a transient system simulation program. Volume 5, Mathematical Reference*, 2007.

[11] G. Nellis and S. Klein. *Heat Transfer.* Cambridge University Press, New York, New York, USA, 2009.

REPORT DOCUMENTATION PAGE	*Form Approved* *OMB No. 0704-0188*

1. REPORT DATE *(DD-MM-YYYY)*
October 2010

2. REPORT TYPE
Conference Paper

3. DATES COVERED *(From - To)*

4. TITLE AND SUBTITLE
A Detailed Physical Trough Model for NREL's Solar Advisor Model: Preprint

5a. CONTRACT NUMBER
DE-AC36-08GO28308

5b. GRANT NUMBER

5c. PROGRAM ELEMENT NUMBER

6. AUTHOR(S)
Michael J. Wagner, Nate Blair and Aron Dobos

5d. PROJECT NUMBER
NREL/CP-5500-49368

5e. TASK NUMBER
SS10.1210

5f. WORK UNIT NUMBER

7. PERFORMING ORGANIZATION NAME(S) AND ADDRESS(ES)
National Renewable Energy Laboratory
1617 Cole Blvd.
Golden, CO 80401-3393

8. PERFORMING ORGANIZATION REPORT NUMBER
NREL/CP-5500-49368

9. SPONSORING/MONITORING AGENCY NAME(S) AND ADDRESS(ES)

10. SPONSOR/MONITOR'S ACRONYM(S)
NREL

11. SPONSORING/MONITORING AGENCY REPORT NUMBER

12. DISTRIBUTION AVAILABILITY STATEMENT
National Technical Information Service
U.S. Department of Commerce
5285 Port Royal Road
Springfield, VA 22161

13. SUPPLEMENTARY NOTES

14. ABSTRACT *(Maximum 200 Words)*
Solar Advisor Model (SAM) is a free software package made available by the National Renewable Energy Laboratory (NREL), Sandia National Laboratory, and the US Department of Energy. SAM contains hourly system performance and economic models for concentrating solar power (CSP) systems, photovoltaic, solar hot-water, and generic fuel-use technologies. Versions of SAM prior to 2010 included only the parabolic trough model based on Excelergy. This model uses top-level empirical performance curves to characterize plant behavior, and thus is limited in predictive capability for new technologies or component configurations. To address this and other functionality challenges, a new trough model derived from physical first principles was commissioned to supplement the Excelergy-based empirical model. This new "physical model" approaches the task of characterizing the performance of the whole parabolic trough plant by replacing empirical curve-fit relationships with more detailed calculations where practical.

15. SUBJECT TERMS
parabolic trough; SAM; solar advisor model; CSP

16. SECURITY CLASSIFICATION OF:			17. LIMITATION OF ABSTRACT	18. NUMBER OF PAGES	19a. NAME OF RESPONSIBLE PERSON
a. REPORT	b. ABSTRACT	c. THIS PAGE			
Unclassified	Unclassified	Unclassified	UL		19b. TELEPHONE NUMBER (*Include area code*)

Standard Form 298 (Rev. 8/98)
Prescribed by ANSI Std. Z39.18

F1147-E(10/2008)